

Supplementary information

Regulating coordination geometry of polyhedron in zero-dimensional metal halides towards tunable emission

Zhipeng Zhang[‡], Jin-Feng Liao^{‡*}, Guichuan Xing^{*}

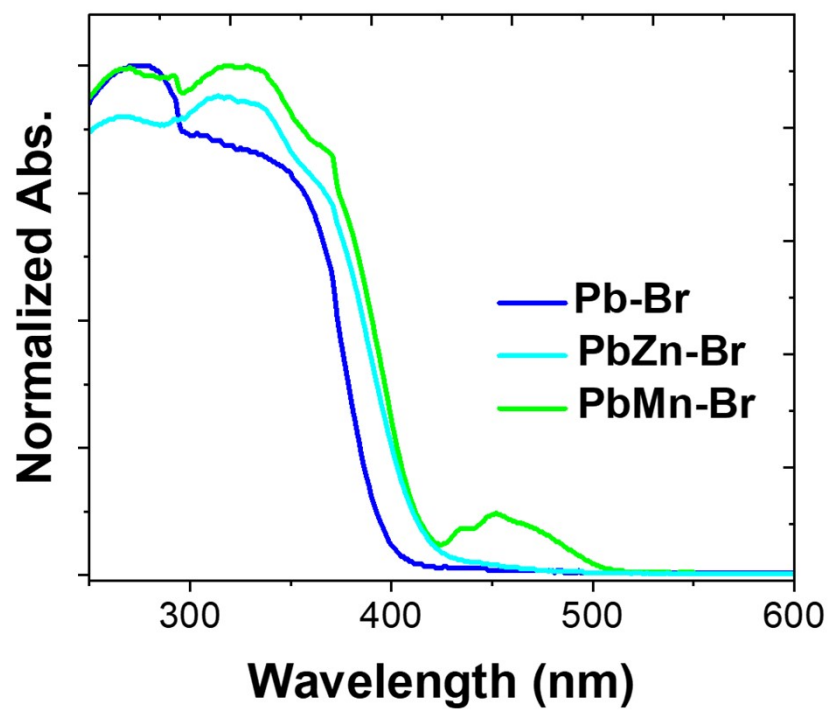


Fig. S1. UV-vis light absorption spectra of Pb-Br, PbZn-Br and PbMn-Br.

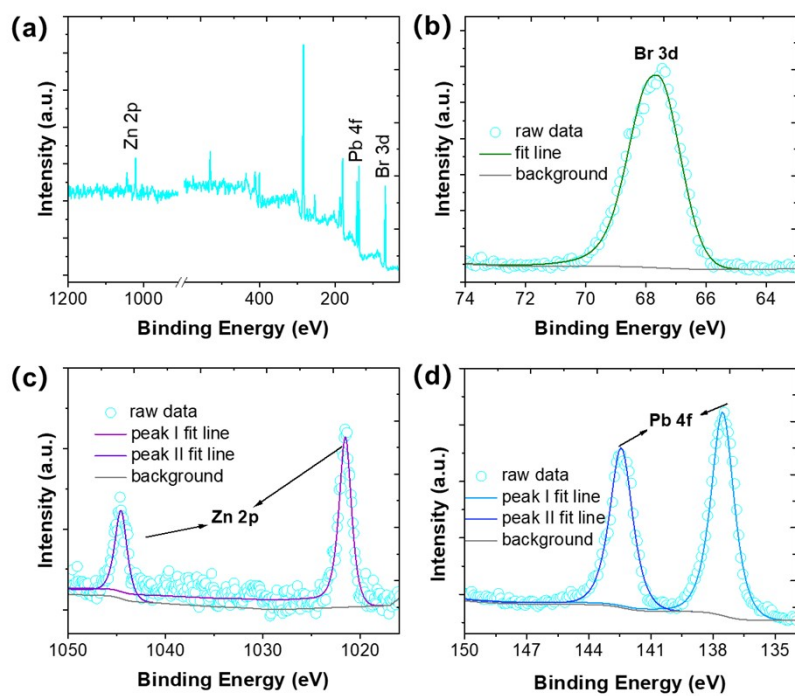


Fig. S2. (a) XPS survey, (b) Br 3d, (c) Zn 2p and (d) Pb 4f spectra of PbZn-Br.

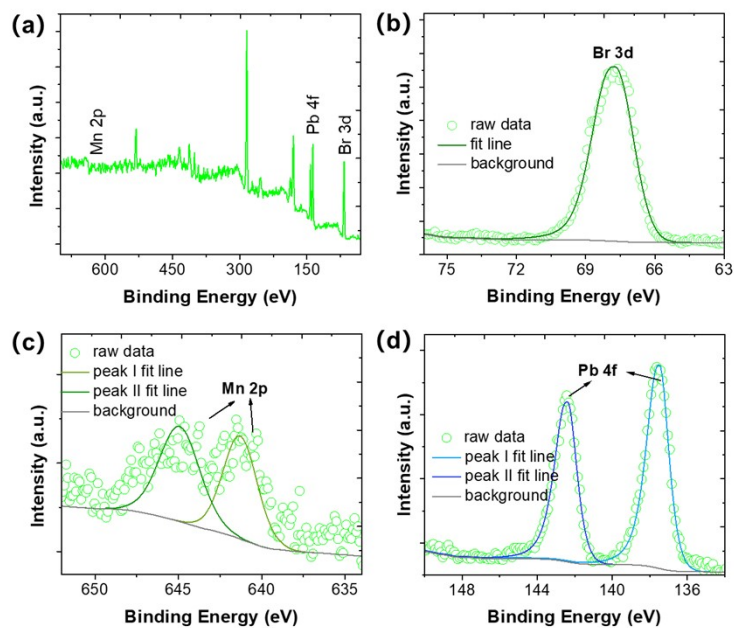


Fig. S3. (a) XPS survey, (b) Br 3d, (c) Mn 2p and (d) Pb 4f spectra of PbMn-Br.

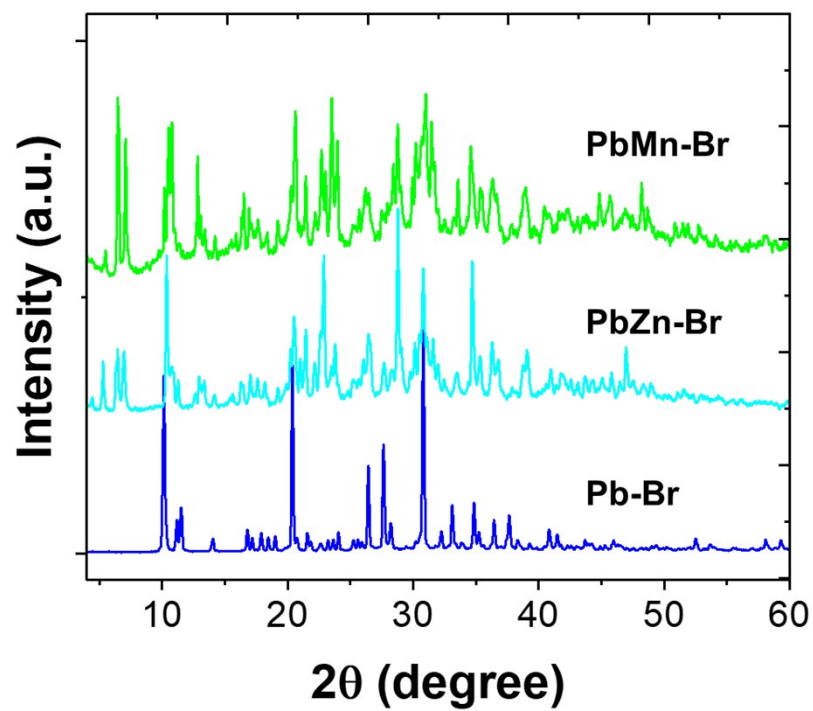


Fig. S4. Powder X-ray diffraction pattern of Pb-Br, PbZn-Br and PbMn-Br.

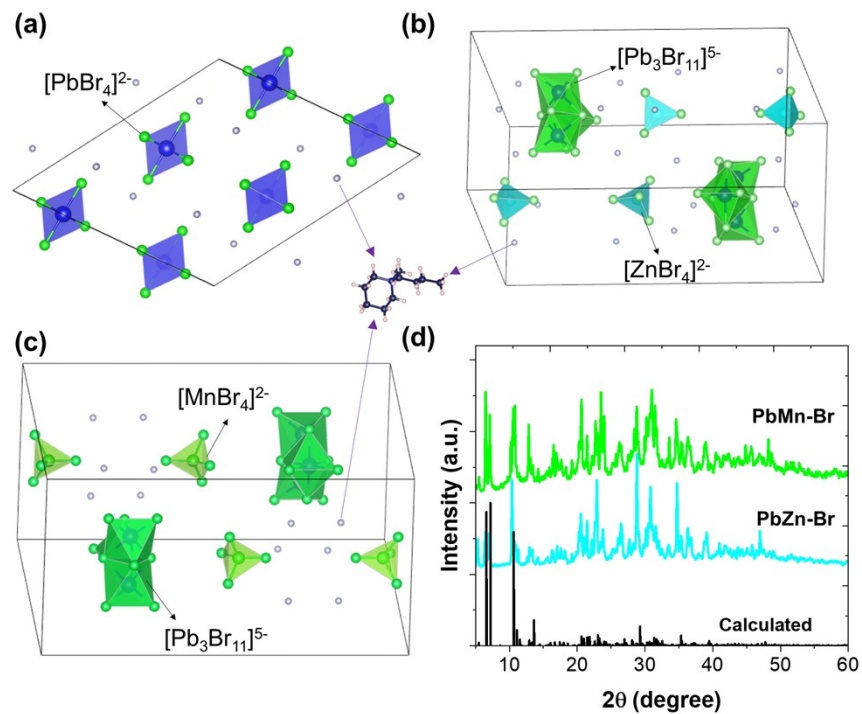


Fig. S5. Schematic view of the organic cation and ionic inorganic polyhedrons in a unit cell of (a) Pb-Br, (b) PbZn-Br and (c) PbMn-Br. (d) Comparison of the experimental powder X-ray diffraction pattern of PbZn-Br and PbMn-Br with the calculated result.

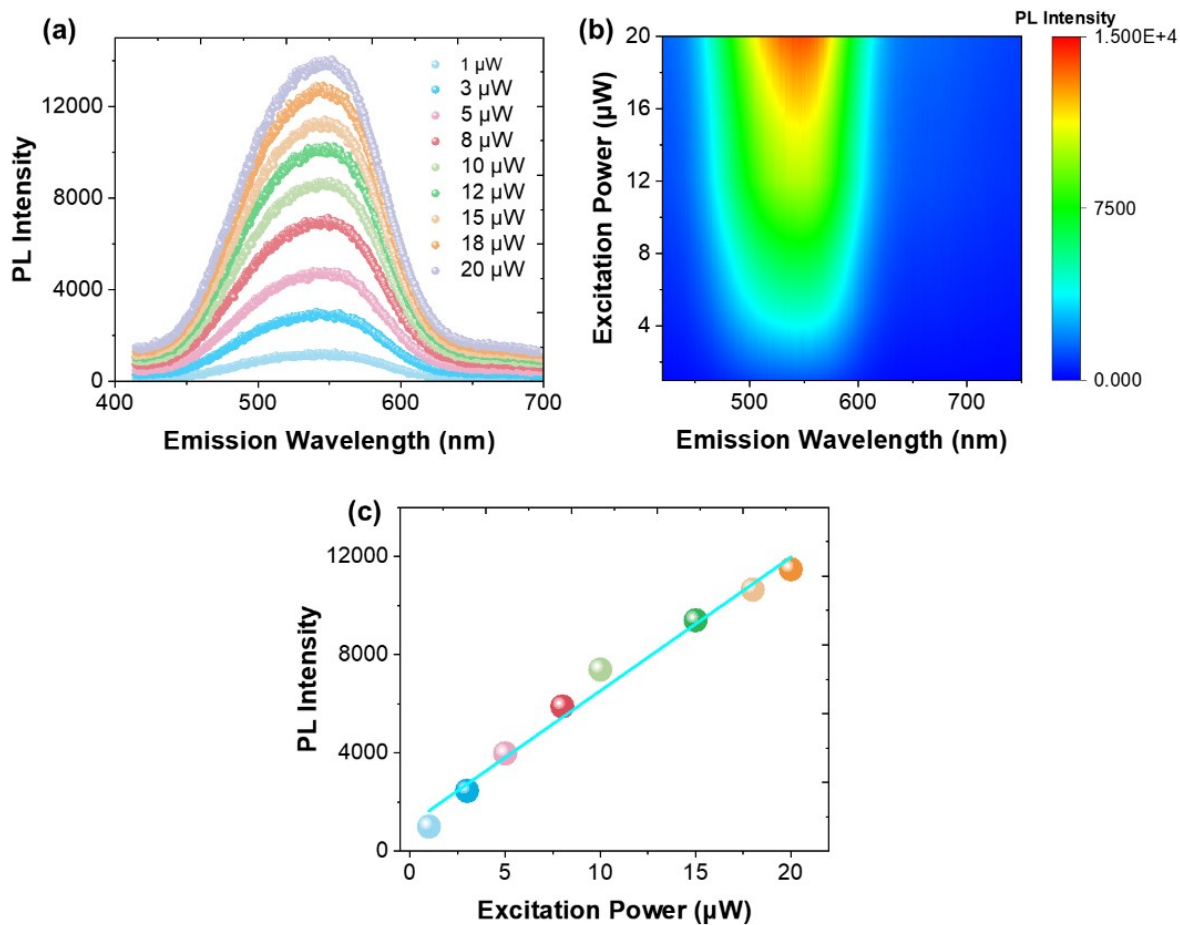


Fig. S6. (a) Excitation power dependent PL emission spectra of PbZn-Br. (b) The emission intensity of photoluminescence plotted as a function of excitation power.

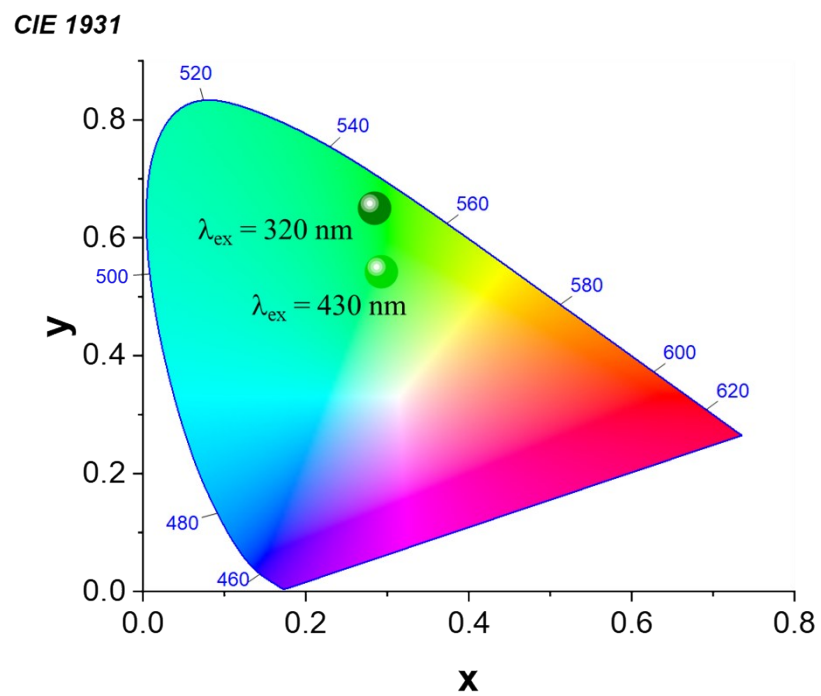


Fig. S7. CIE coordinates of PbMn-Br under excitation at 320 nm and 430 nm.

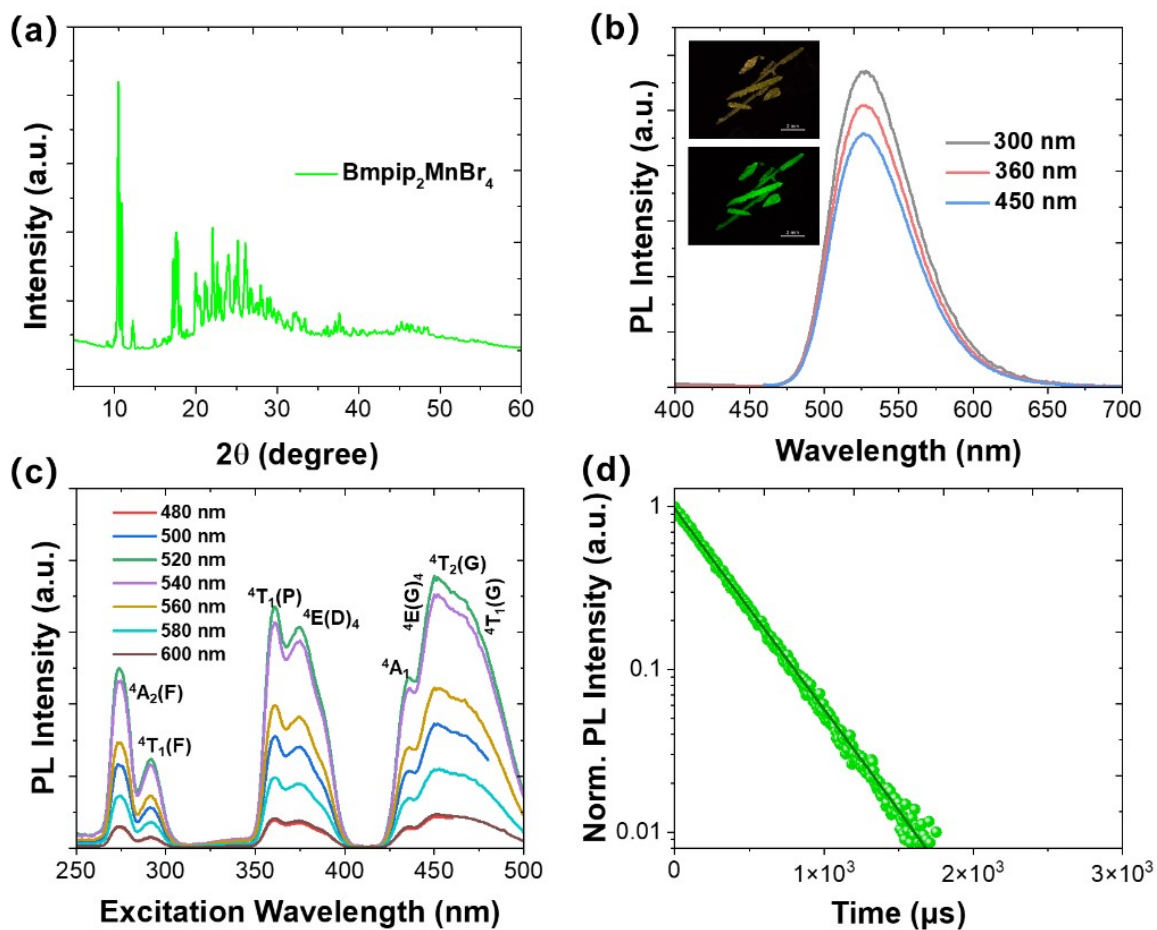


Fig. S8. Characterizations of $\text{Bmpip}_2\text{MnBr}_4$. (a) Powder XRD diffraction pattern. (b) PL emission spectra under excitation at 300 nm, 360 nm and 450 nm. Inset are the optical photographs of the single crystals under the conditions of natural light and UV irradiation (365 nm). (c) PLE spectra. (d) Time resolved PL emission decay.

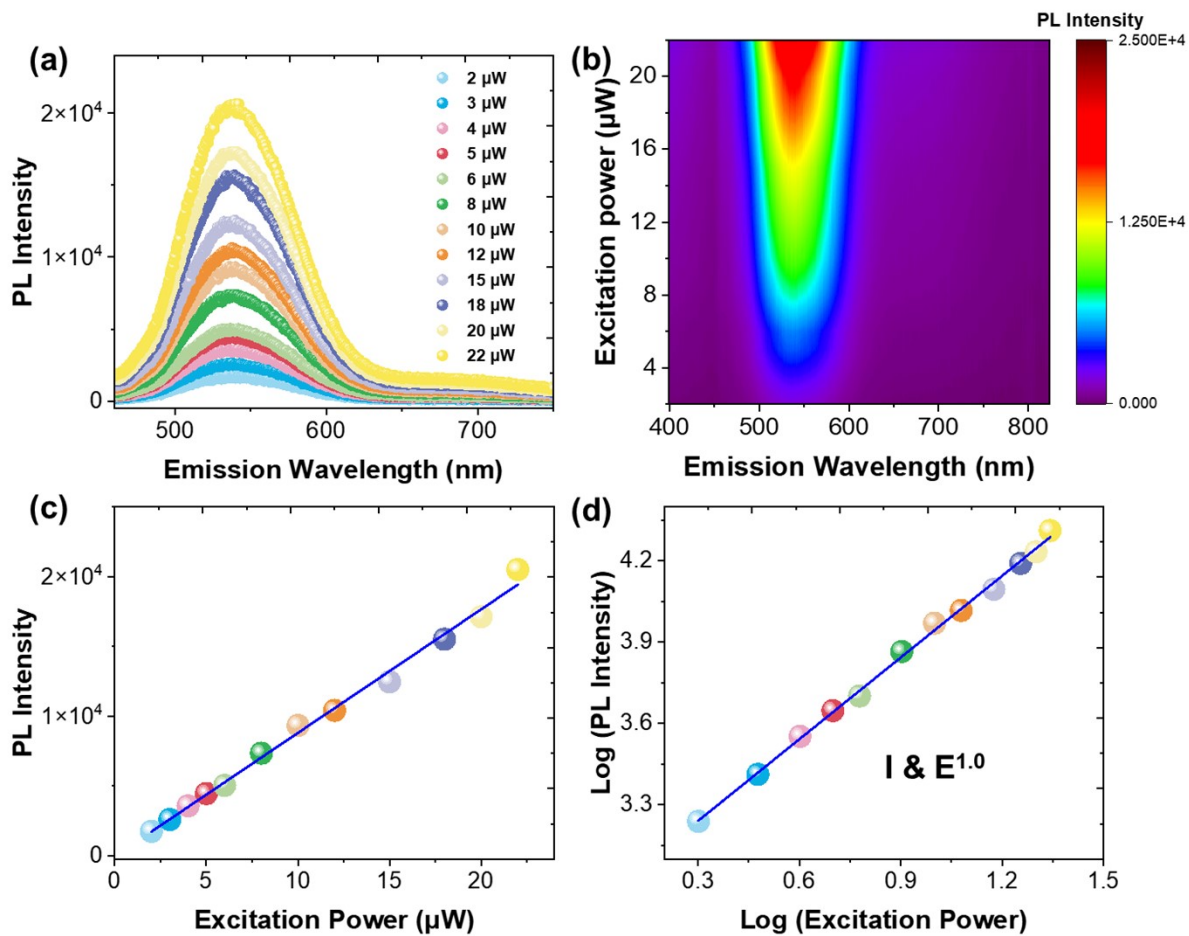


Fig. S9. (a) Excitation power dependent PL emission spectra of PbMn-Br. (b) Pseudocolor map of excitation power dependent emission spectra of PbMn-Br. (c) The emission intensity of photoluminescence plotted as a function of excitation power. (d) The plot of Log (PL Intensity) as a function of excitation power.

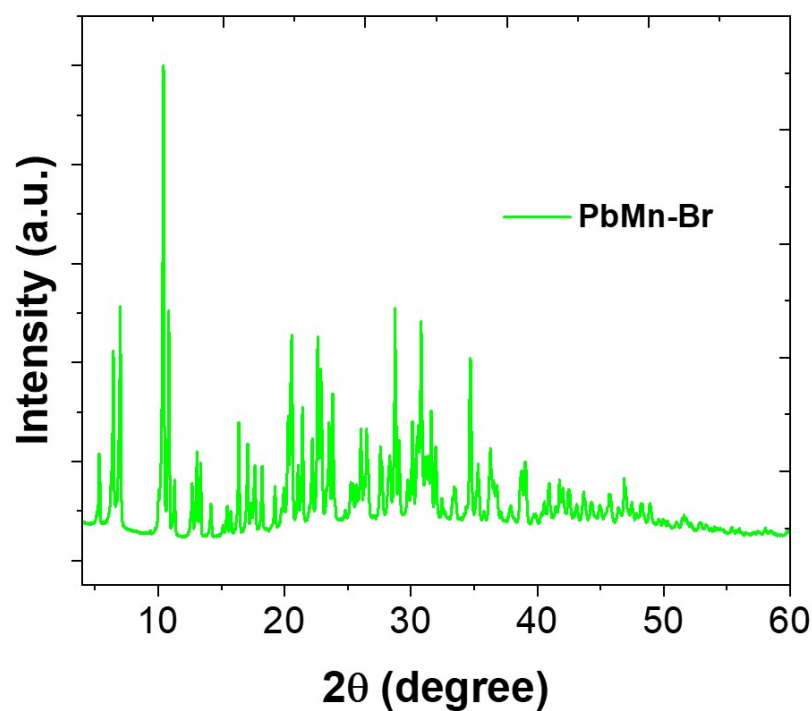


Fig. S10. Powder X-ray diffraction pattern of PbMn-Br after exposure in air for one year.

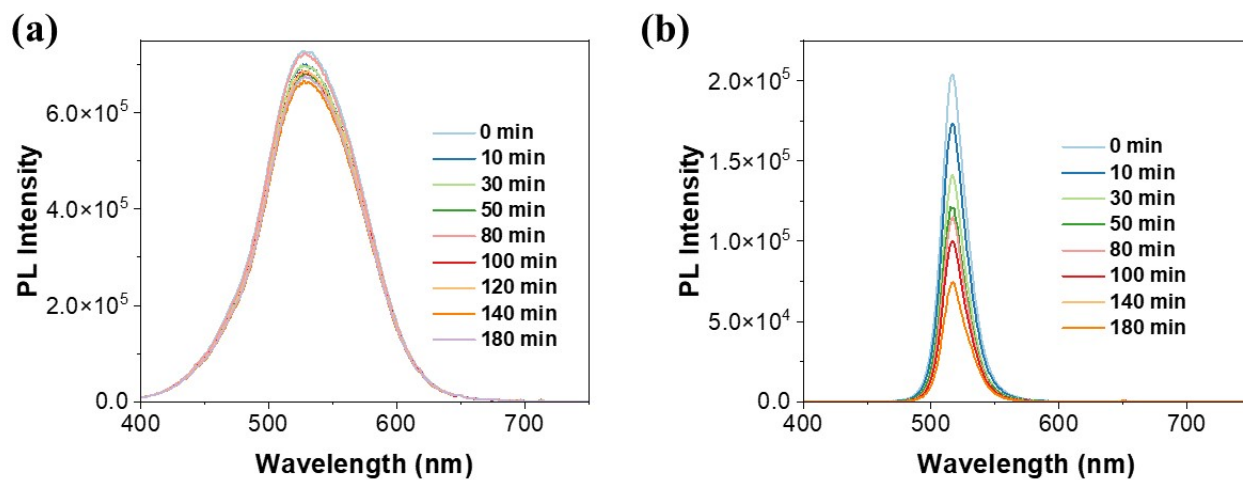


Fig. S11. PL emission spectra of (a) PbMn-Br and (b) CsPbBr₃ as a function of heat duration at 80°C.

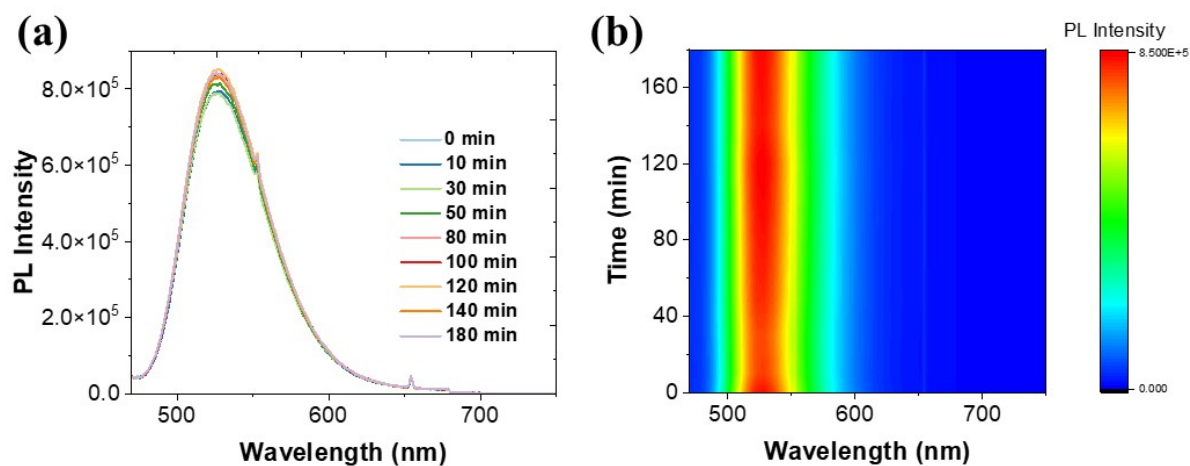


Fig. S12. (a) PL emission spectra and (b) pseudocolor map of time-dependent PL intensity of 450-nm-excited PbMn-Br under the heating of 80°C.

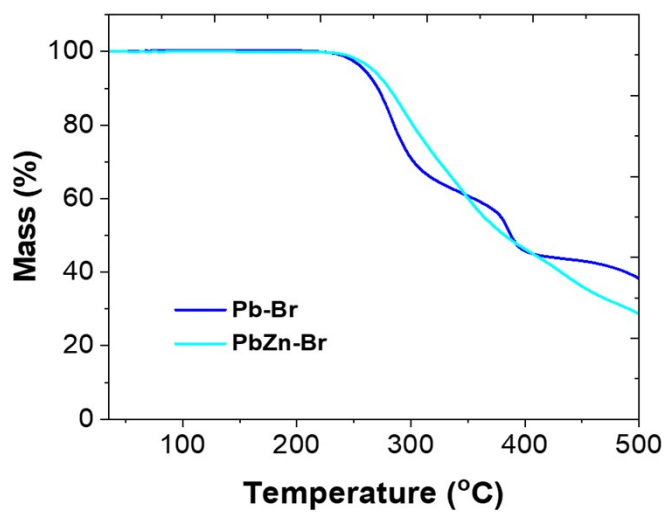


Fig. S13. Thermo-gravimetric analysis curves of Pb-Br and PbZn-Br.

Table S1. Crystal data and structure refinements for (Bmpip)₂[PbBr₄], (Bmpip)₉[Pb₃Br₁₁](ZnBr₄)₂ and (Bmpip)₉[Pb₃Br₁₁](MnBr₄)₂.

Compound	(Bmpip) ₂ [PbBr ₄]	(Bmpip) ₉ [Pb ₃ Br ₁₁](ZnBr ₄) ₂	(Bmpip) ₉ [Pb ₃ Br ₁₁](MnBr ₄) ₂
Crystal system	Monoclinic	Hexagonal	Trigonal
Space group	C 2/c	P 63/m	P 31/c
Unit cell dimensions	a = 20.4084 Å	a = 15.1977 Å	a = 15.2330 Å
	b = 8.4516 Å	b = 15.1977 Å	b = 15.2330 Å
	c = 18.5924 Å	c = 31.6698 Å	c = 31.8165 Å
	α = 90.0000°	α = 90.0000°	α = 90.0000°
	β = 122.1860°	β = 90.0000°	β = 90.0000°
	γ = 90.0000°	γ = 120.0000°	γ = 120.0000°
Volume (Å ³)	2714.06	6334.78	6393.724

Table S2. Photophysical property comparison between some reported multi-ionic metal halides.

	PL Peak [nm]	PLQY [%]	Lifetime	Ref.
(C ₉ NH ₂₀) ₉ [Pb ₃ Br ₁₁](MnBr ₄) ₂	565	15.6	27.43 ns	1
(C ₉ NH ₂₀) ₉ [Pb ₃ Br ₁₁](FeBr ₄) ₂	565	2.44	3.95 ns	1
(C ₉ NH ₂₀) ₉ [Pb ₃ Br ₁₁](CoBr ₄) ₂	565	1.16	8.02 ns	1
(C ₉ NH ₂₀) ₉ [Pb ₃ Br ₁₁](ZnBr ₄) ₂	565	8.1	35.69 ns	1
(HMTA) ₄ PbMn _{0.69} Sn _{0.31} Br ₈	460, 550, 645	73	85 ns, 427 μs, 3.4 μs	2
(C ₁₀ NH ₂₂) ₂ Pb _{1-x} Sn _x Br ₄	470, 670	43.3	77 ns, 6 μs	3
(bmpy) ₉ [ZnBr ₄] ₂ [Pb ₃ Br ₁₁]	564	7	36 ns	4
(C ₉ NH ₂₀) ₉ Pb ₃ Zn ₂ Br ₁₉	565	8.1	42 ns	5
Cs ₄ MnBi ₂ Cl ₁₂	610	25.7	144 μs	6
(Bmpip) ₂ Pb _x Sn _{1-x} Br ₄	470, 670	39	63.35 ns, 6.13 μs	7
(bmpy) ₉ [ZnCl ₄] ₂ [Pb ₃ Cl ₁₁]	512	~100	540 ns	8
PbMn-Br	534, 527	11, 67	36 ns, 240 μs	this work
PbZn-Br	527	9	38 ns	this work

References:

1. M. Li, M. S. Molokeev, J. Zhao and Z. Xia, *Adv. Opt. Mater.*, 2020, **8**, 1902114.
2. L.-J. Xu, S. Lee, X. Lin, L. Ledbetter, M. Worku, H. Lin, C. Zhou, H. Liu, A. Plaviak and B. Ma, *Angew. Chem. Int. Ed.*, 2020, **59**, 14120-14123.
3. J.-F. Liao, Z. Zhang, J.-H. Wei, Z.-Z. Zhang, B. Wang, L. Zhou, G. Xing, Z. Tang and D.-B. Kuang, *Adv. Opt. Mater.*, 2022, **10**, 2102426.
4. S. Lee, C. Zhou, J. Neu, D. Beery, A. Arcidiacono, M. Chaaban, H. Lin, A. Gaiser, B. Chen, T. E. Albrecht-Schmitt, T. Siegrist and B. Ma, *Chem. Mater.*, 2020, **32**, 374-380.
5. M. Li, Y. Li, M. S. Molokeev, J. Zhao, G. Na, L. Zhang and Z. Xia, *Adv. Opt. Mater.*, 2020, **8**, 2000418.
6. J.-H. Wei, J.-F. Liao, X.-D. Wang, L. Zhou, Y. Jiang and D.-B. Kuang, *Matter*, 2020, **3**, 892-903.
7. L. Fan, K. Liu, Q. Zeng, M. Li, H. Cai, J. Zhou, S. He, J. Zhao and Q. Liu, *ACS Appl. Mater. Interfaces*, 2021, **13**, 29835-29842.
8. C. Zhou, H. Lin, J. Neu, Y. Zhou, M. Chaaban, S. Lee, M. Worku, B. Chen, R. Clark, W. Cheng, J. Guan, P. Djurovich, D. Zhang, X. Lü, J. Bullock, C. Pak, M. Shatruk, M.-H. Du, T. Siegrist and B. Ma, *ACS Energy Lett.*, 2019, **4**, 1579-1583.